

Hard X-ray dosimetry of a plasma focus suitable for industrial radiography

P. Knoblauch^a, V. Raspa^a, F. Di Lorenzo^a, A. Clause^b, C. Moreno^{a,*}

^a Universidad de Buenos Aires, Depto. de Física, FCEN, Instituto de Física del Plasma (INFIP) - CONICET, and PLADEMA-CNEA. Pab. 1, Ciudad Universitaria, 1428 Buenos Aires, Argentina

^b Universidad Nacional del Centro, PLADEMA-CNEA and CONICET, Campus Universitario, Paraje Arroyo Seco, 7000 Tandil, Buenos Aires, Argentina

A B S T R A C T

Dosimetric measurements of the hard X-ray emission by a small-chamber 4.7 kJ Mather-type plasma focus device capable of producing neat radiographs of metallic objects, were carried out with a set of thermoluminescent detectors TLD 700 (LiF:Mg,Ti). Measurements of the hard X-ray dose dependence with the angular position relative to the electrodes axis, are presented. The source-detector distance was changed in the range from 50 to 100 cm, and the angular positions were explored between $\pm 70^\circ$, relative to the symmetry axis of the electrodes. On-axis measurements show that the X-ray intensity is uniform within a half aperture angle of 6° , in which the source delivers an average dose of (1.5 ± 0.1) mGy/sr per shot. Monte Carlo calculations suggest that the energy of the electron beam responsible for the X-ray emission ranges 100–600 keV.

1. Introduction

Plasma focus derived X-ray sources may find potential applications in medicine and industry, because they present a compact, low cost solution that offers performances in terms of intensity and exposure time. During the last decades plasma focus devices were intensively investigated as pulsed X-ray sources suitable for many novel radiographic applications (Dubrovsky et al., 2000, 2006; Castillo et al., 2001, 2008; Da Re et al., 2001; Hussain et al., 2003a, 2003b, 2004, 2005; Bogolubov et al., 2009; Verma et al., 2010; Moreno et al., 2002; Venere et al., 2001; Pavez et al., 2012). The operation principle of plasma focus devices lies in the use of energy stored in a capacitor bank to create a low density plasma that is electromagnetically accelerated and subsequently compressed by the Lorentz force associated with the discharge current (pinch). During the pinch phase, an intense collimated beam of relativistic electrons is usually emitted towards the anode, lasting the time of the pinch, typically a few tenths of nanoseconds (Ceccolini et al., 2011). Hard X-rays are produced by impact of runaway electrons on a metallic target usually located inside the (hollow) anode, which typically is also the central electrode of the discharge (Tartari et al., 2004). The spectrum of the X-rays, generated by collisions of the electron beam with a target, was determined indirectly in the past by differential absorption-based techniques (Raspa and Moreno, 2009; Raspa et al., 2010). The spectrum presents a single dominant peak around 75 keV and a spectral bandwidth covering the 40–200 keV region (Raspa et al., 2004, 2008; Moreno et al., 2006, 2007).

In order to have commercially competitive devices, information

about the distribution of the radiation dose in the application region is important either from the point of view of radiation protection or the design of radiographic procedures. Castillo et al. (2001) used TLDs to measure the hard X-ray dose for energies above 25 keV in a 2 kJ 31 kV plasma focus. They found that at a distance of 1 m from the focus, the hard X-ray dose on axis is about 0.1 mrad per shot, not varying for half aperture angles smaller than 5° from the electrodes axis. More recently and also by using TLDs, Castillo et al. (2007) determined that the X-ray emission of a 4.8 kJ 37 kV plasma focus shows a bimodal angular distribution peaked at 20° from the electrodes axis, for emitted photons of energies above 15 keV. Krása et al. (2002) performed a semiconductor and thermoluminescent dosimetry of the soft X-ray emissions of a plasma focus. Fabbri et al. (2007) performed an analysis of radiation protection of a plasma focus used for medical applications, suggesting several safety operational criteria. Whitlock et al. (2002) measured the X-ray spectrum of a plasma focus operating at 60 Hz using a convex curved-crystal spectrograph. Tafreshi et al. (2010) studied the anisotropy in X-ray production and the absorbed X-ray dose in the Sahand PF device using TLDs. The study showed that the X-ray production is isotropic within the experimental resolution, and that a 2-mm iron shield has a considerable role in decreasing the absorbed dose. Angeli et al. (2006) used LiF TLD dosimeters and a differential attenuation technique to determine the X-ray spectrum of a 7 kJ 17 kV plasma focus, finding a peak energy of 10 keV. El-Aragi et al. (2010) measured the X-ray dose in a 100 J plasma focus device operated with different gases and pressures, using a time-integrated thermoluminescence TLD 500 dosimeters. Tartari et al. (2004) designed a PF device to produce X-rays

* Corresponding author.

E-mail address: moreno@df.uba.ar (C. Moreno).

for brachytherapy by impinging the back electron beam on high Z targets. They estimated that the dose rate delivered in a LiF dosimeter at 10 mm from the X-ray source was around 4.5 Gy/shot, which makes it suitable for radiosurgery. Recently, Zapryanov et al. (2011) determined that the average dose of the X-ray emission in a 3 kJ 18 kV, plasma focus is a few tenth of Sv per shot.

In general, pulsed photon radiation fields are currently a matter of growing interest in applied radiology. Klammer et al. (2012) recently presented a novel X-ray reference field for pulsed photon radiation for medical applications. Radiation protection dosimeters are usually tested in continuous fields, although Ankerhold et al. (2009) pointed out the deficiencies of active electronic radiation protection dosimeters in pulsed fields. Actually, standards for the calibration and use of dosimeters in pulsed radiation fields is still a matter of study and preparation (ISO, 2012; IEC, 2012). Therefore, the X-rays emissions of plasma focus designed as pulsed radiation sources are promising candidates for reference studies.

In the present article, dosimetric measurements of the hard X-ray output of a small-chamber 4.7 kJ 30 kV Mather-type PF device, especially designed for radiographic applications, are presented. The measurements were performed using TLD 700 detectors, which are practically insensitive to the neutrons produced when operating with deuterium. The dose in the spatial region where the best radiographic images were obtained was carefully mapped using a tight array of detectors.

2. Experimental setup

The experimental setup is shown in Fig. 1. The facility is the plasma focus GN1, powered by a capacitor bank composed by fifteen 0.7 μF capacitors Maxwell 31161, connected in parallel and charged up to 30 kV (4.7 kJ of stored energy). Peak currents of 340 kA can be driven in a quarter-period of 1.23 μs . The coaxial gun is composed by a hollow anode made of copper, surrounded by a squirrel-cage-like bronze cathode. The anode is a tube of 85 mm in length and 38 mm outer diameter, being the wall 2-mm-thick. The cathode is formed by eight brass rods of 3 mm outer diameter (OD) and 87 mm long, disposed equally spaced on a circle of 37 mm in diameter. The electrodes are separated by a Pyrex sleeve of 50 mm OD, 4 mm thick and 34 mm long. The set is coaxially located inside a 2-mm-thick stainless-steel cylindrical chamber.

In Mather-type plasma focus devices there are two sources of X-rays: soft X-rays are produced inside the pinch and hard X-rays are produced in the back of the anode. In the present study only the latter were measured, which result from the impact of relativistic electron beams originated in the pinch zone and accelerated backwardly along the anode axis. These X-rays beams are of great interest for radiographic applications for their intensity and short duration (tens of nanoseconds). Fig. 2 shows radiographs of a car spark plug and a drill inserted in a piece of copper both obtained with a single GN1 shot, locating the objects at 1-m distance from the chamber front end. The present device

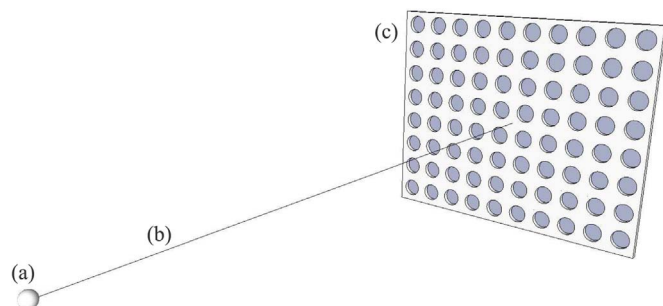


Fig. 1. Sketch of the experimental setup to measure the hard X-ray dose on the electrodes axis. (a) Hard X-ray source; (b) electrodes axis; (c) 8×10 , plastic encased, TLDs array.

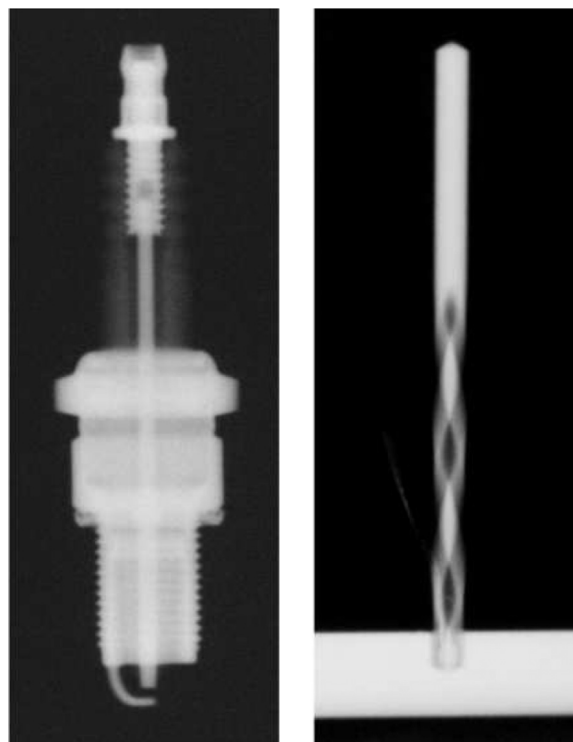


Fig. 2. Single shot radiographic images of a spark plug and a drill inserted in a piece of copper.

was operated using a total pressure of 3.5 mbar of a deuterium-argon mixture (2.5% of argon by volume) as working gas, since it maximizes the hard X-ray production and the shot to shot regularity for this device. The output window of the hard X-ray radiation is a 0.75 mm thick stainless steel flat disk, which is also the front end of the discharge chamber. Additional details of the device can be found elsewhere (Moreno et al., 2002, 2000). A non integrating Rogowski coil and a photomultiplier tube coupled to a 5 cm thick and 5 cm in diameter NE102A plastic scintillator were used to monitor the discharge. The assembly was placed 3.9 m away from the chamber, inside a Faraday cage to reduce noise pickup.

Thermoluminescent detectors Harshaw TLD 700 from Bicon were used to measure the hard X-ray dose. They are lithium fluoride crystals doped with magnesium and titanium impurities (LiF:Mg,Ti), mainly enriched with ^7Li (99.93% of ^7Li and 0.07% of ^6Li). The preponderance of ^7Li makes the detectors practically insensitive to the neutrons that can be emitted during the focalization. The low dependence of the measured dose on the energy of the detected electromagnetic radiation (Luo and Velbeck, 2002), is another advantage of using TLD 700. The physical dimensions of each detector are: $3 \times 3 \times 0.89$ mm rectangular prism. To ensure the CPE (Charged-Particle Equilibrium) condition during the measurements, the detectors were placed inside suitable plastic containers. The dosimeters were calibrated for gamma-rays using a certified ^{137}Cs source. At the time of the experiment, the dose equivalent rate at 1 m from the source, at 101.4 kPa and 23.7 $^{\circ}\text{C}$ ambient pressure and temperature, respectively, as endorsed by the Argentine Nuclear Regulatory Commission, was 73.94 Gy/min. The following protocol was repeated three times to obtain the calibration factor relating the total thermoluminescent signal with the dose:

1. Prior to the irradiation, the TLDs are submitted to 1-h annealing in an oven at 400 $^{\circ}\text{C}$ followed by 3 h at 100 $^{\circ}\text{C}$.
2. The dosimeter batch is exposed 30 min at 1 m from the standard source.
3. After irradiation, the TLDs are placed in an oven at 100 $^{\circ}\text{C}$ during 30 min to eliminate porosity-dependent humidity effects.

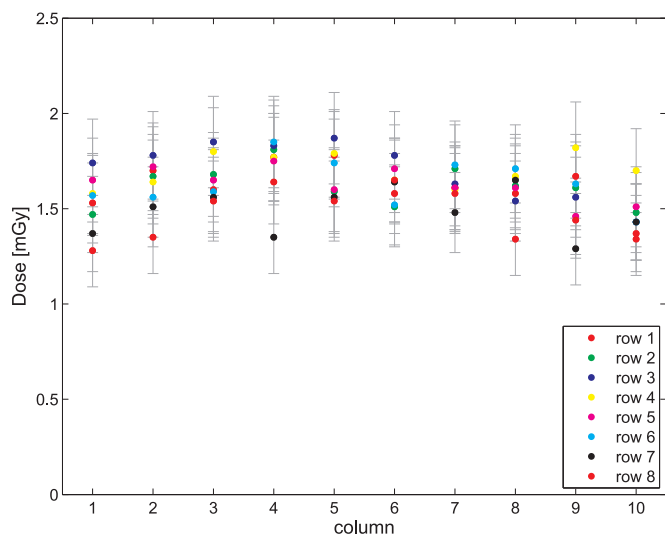


Fig. 3. Hard X-ray dose measured for angular positions near the axis, 53 cm away from the source. Thirty plasma focus shots were accumulated.

- In order to minimize humidity in the reader, 99.995%-pure dry nitrogen is circulated through the instrument for 20 min.
- The recordings of the glow curve are performed with an automatic TLD-Reader (model: QS3500, manufacturer: Harshaw/Bicron Inc., USA). The readout heating is defined according to the provider specifications: from 110 °C to 350 °C with 5 °C/s ramp rate.

As a selection criteria, the TLD detectors used verify that under controlled irradiation conditions, the individual measurements were reproducible and also consistent with readings from any other element of the set. The dose uncertainty was estimated as 6%, from the standard deviation of the individual readings.

3. Hard X-ray dosimetry

Since the radiation emitted on axis is the one generally used for radiographic applications, the uniformity of the hard X-ray dose for angular positions near the electrodes axis was investigated considering a typical object-source configuration. Measurements were carried out using an 8 × 10 rectangular array of TLD 700 dosimeters, centered on the electrodes axis and positioned at 53 cm away from the source. Fig. 3 shows the dose registered by each detector as a function of the corresponding angular position of each column of the array, after being irradiated with 30 plasma focus shots. The dispersion between the dose registered by the detectors placed on different columns of the array is below the measurement uncertainty. The same observation can be made for the dose associated to different rows. Accordingly, the on axis absorbed dose was determined from the average of the individual measurements.

Regarding that each point in Fig. 3 corresponds to the accumulated dose of 30 shots, a hard X-ray dose of $(53 \pm 3) \mu\text{Gy}/\text{shot}$ on axis at 53 cm from the source is calculated. These measurements additionally show that the corresponding uniform irradiation cone has a half aperture angle of 6°. The hard X-ray dose per shot on the electrodes axis was also measured at 73 and 93 cm from the source, and the $1/r^2$ dependence between the dose and the source-detector distance (r), was checked.

The angular distribution of the dose was investigated also by using TLD 700 dosimeters. The detectors were placed concentrically with the source position (Di Lorenzo et al., 2007), at two different radial distances from the source: 54 and 74 cm, respectively, as sketched in Fig. 4. The hard X-ray source is located inside the anode tube, centered on axis, at 6 cm from the anode open end where a lead target was

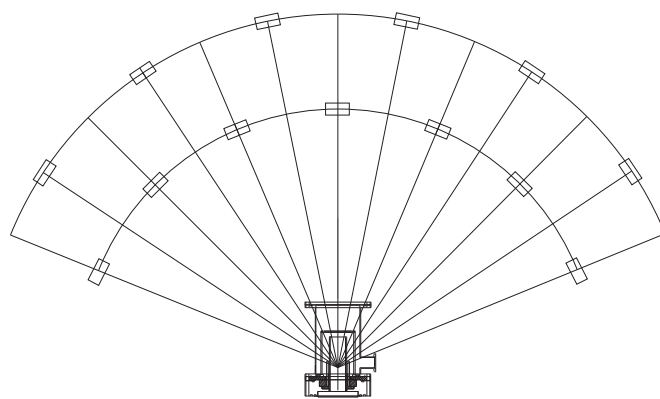


Fig. 4. Experimental setup for the measurements of the dose angular profile. The TLDs were placed concentrically with the source position.

placed. This kind of target configuration inside the anode is the one we normally use to enhance the X-ray production and collimation. The angular positions were explored between $\pm 70^\circ$ relative to the symmetry axis of the electrodes. The detectors were irradiated with 40 plasma focus shots. The emission was found to be anisotropic and collimated, having a dominant peak on the electrodes axis, and a $\pm 20^\circ$ angle range where the dose symmetrically decays to 20% of its central value (see Fig. 5).

In order to elucidate the experimental results, Monte Carlo simulations were performed using the MCNP5 code (Briesmeister, 2000). The experimental setup was modelled in full detail including floor, walls, chamber and its internal structure, and the lead target. The dose absorbed by each detector was calculated assuming narrow electron beams with energies ranging 100–600 keV colliding with the lead target. Fig. 5 compares the numerical doses obtained averaging 10^8 events with the experimental data, showing excellent agreement. Moreover, the calculated X-ray spectrum (see Fig. 6) is consistent with experimental measurements from differential attenuation on metallic filters performed for the same device and reported in Raspa et al. (2010, 2004).

4. Conclusions

Dosimetric measurements were used to investigate the angular distribution of the hard X-ray output of a 4.7 kJ 30 kV plasma focus device, exploring angular positions between $\pm 70^\circ$ relative to the electrodes axis. Measurements show that the major fluency of radiation was detected on the electrodes axis, and determine a $\pm 20^\circ$ range where the dose symmetrically decays from its central value.

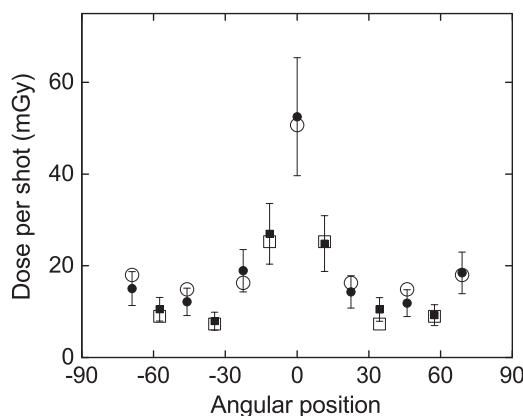


Fig. 5. Angular distribution of the hard X-ray dose per shot, measured at 54 cm (circles) and 74 cm (squares) from the source. The symbols refer to the experiment (solid) and MCNP Monte Carlo simulation (empty).

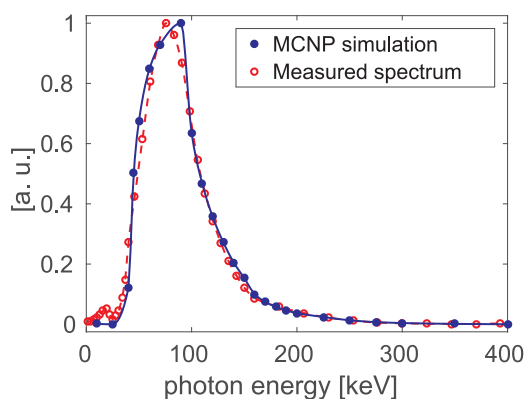


Fig. 6. X-ray spectrum calculated with a Monte Carlo code assuming narrow electron beams with energies ranging 100–600 keV colliding with the lead target (continuous line). The measured spectrum is also shown (dashed line) (Raspa et al., 2010). The spectra are normalized by their maxima.

A dose per shot of $(53 \pm 3) \mu\text{Gy}$ was registered on axis at 53 cm from the hard X-ray source, which is a typical object-source configuration for single shot radiographic applications. Additionally, the irradiation was found to be uniform for angular positions within the $\pm 6^\circ$ range.

Monte Carlo calculations allowed to infer electron beams energies up to 600 keV to reproduce the measured angular distribution of the hard X-ray dose.

The collimation imposed by the anode tube produces a narrow radiation beam of small aperture angle, providing a pulsed intense hard X-ray source with strong directionality, all features that can benefit applications.

Even if the device operator was placed on the axis at 53 cm from the source, a thousand plasma focus shots with hard X-ray production would be required to exceed the average annual limit of 20 mSv effective dose on a 5 years period, under the condition that the limit of 50 mSv is not exceeded in any individual year, as determined by International Commission on Radiation Protection (2007).

Acknowledgements

This work was supported by UBA (Proj. X152), and CONICET (1220090101055CO). C.M. and A.C. are members of CONICET.

References

Angeli, E., Bonifazzi, C., Da Re, A., Marziani, M., Tartari, A., Frignani, M., Mannucci, S., Mostacci, D., Rocchi, F., Sumini, M., 2006. *Nukleonika* 51 (1), 15–20.
 Ankerhold, U., Hupe, O., Ambrosi, P., 2009. *Radiat. Prot. Dosim.* 135 (3), 149–153.
 Bogolubov, Ye.P., Koltunov, M.V., Lemeshko, B.D., Mikerov, V.I., Samosyuk, V.N., Sidorov, P.P., Yurkov, D.I., 2009. *Nucl. Instrum. Methods Phys. Res. Sect. A* 605 (1–2), 62.

Briesmeister, J. 2000. MCNP – A General Monte Carlo N Particle Transport Code, version 4C, Los Alamos National Laboratory, Report LA-13709-M.
 Castillo, F., Milanese, M.M., Moroso, R.L., Pouzo, J.O., Santiago, M.A., 2001. *IEEE Trans. Plasma Sci.* 29 (6), 921.
 Castillo, F., Herrera, J., Gamboa, I., Rangel, J., Golzarri, J., Espinosa, G., 2007. *J. Appl. Phys.* 101 (1), 013303.
 Castillo, F., Gamboa-deBuen, I., Herrera, J.J.E., Rangel, J., Villalobos, S., 2008. *Appl. Phys. Lett.* 92 (5), 051502.
 Ceccolini, E., Rocchi, F., Mostacci, D., Sumini, D., Tartari, A., 2011. *Rev. Sci. Instrum.* 82, 0851031–0851037.
 Da Re, A., Mezzetti, F., Tartari, A., Verri, G., Rapezzi, L., Gribkov, V.A., 2001. *Nukleonika* 46 (1), S123.
 Di Lorenzo, F., Raspa, V., Knoblauch, P., Lazarte, A., Moreno, C., Clausse, A., 2007. *J. Appl. Phys.* 102 (3), 033304.
 Dubrovsky, A.V., Silin, P.V., Gribkov, V.A., Volobuev, I.V., 2000. *Nukleonika* 45 (3), 185.
 Dubrovsky, A.V., Gribkov, V.A., Ivanov, Y.P., Karpinski, L., Orlova, M., Romanova, V.M., Scholz, M., Volobuev, I.V., 2006. *Nukleonika* 51 (1), 21.
 El-Aragi, G., Ayad, M., El-Kolaly, M., Madcour, W., 2010. *Pramana J. Phys.* 75 (4), 727–736.
 Fabbri, A., Frignani, M., Mannucci, S., Mostacci, D., Rocchi, F., Sumini, M., Teodori, F., Angeli, E., Tartari, A., Cucchi, G., 2007. *J. Radiol. Prot.* 27 (4), 465–470.
 Hussain, S., Ahmad, S., Khan, M.Z., Zakaullah, M., 2003a. *J. Fusion Energy* 22 (3), 195.
 Hussain, S., Zakaullah, M., Ali, S., Bhatti, S., Waheed, A., 2003b. *Phys. Lett. A* 319 (1–2), 181.
 Hussain, S., Zakaullah, M., Ali, S., Waheed, A., 2004. *Plasma Sources Sci. Technol.* 6 (3), 2296.
 Hussain, S., Shafiq, M., Ahmad, R., Waheed, A., Zakaullah, M., 2005. *Plasma Sources Sci. Technol.* 14 (1), 61.
 IEC. Radiation Protection Instrumentation – Electronic Counting Dosimeters for Pulsed Fields of Ionizing Radiation. IEC/TS 62743.
 International Commission on Radiation Protection, 2007. The 2007 Recommendations of the International Commission on Radiological Protection. Baltimore: Elsevier; ICRP Publication ICRP 103: Annals of the ICRP 37 (2–4).
 ISO, 2012. Radiological Protection – Characteristics of Reference Pulsed Radiation. ISO/NP TS 18090.
 Klammer, J., Roth, J., Hupe, O., 2012. *Radiat. Prot. Dosim.* 151 (3), 478–482.
 Krása, J., Cejnarová, A., Juha, L., Ry, L., Scholz, M., Kubeš, P., 2002. *Radiat. Prot. Dosim.* 100 (1–4), 429–432.
 Luo, L.Z., Velbeck, K.J., Rotunda, J.E., 2002. *Radiat. Prot. Dosim.* 101 (1–4), 211.
 Moreno, C., Bruzzone, H., Martínez, J., Clausse, A., 2000. *IEEE Trans. Plasma Sci.* 28 (5), 1735.
 Moreno, C., Venere, M., Barbuzza, R., Del Fresno, M., Ramos, R., Bruzzone, H., Florido, P., González, J., Clausse, A., 2002. *Braz. J. Phys.* 32 (1), 20.
 Moreno, C., Raspa, V., Sigaut, L., Vieytes, R., Clausse, A., 2006. *Appl. Phys. Lett.* 89 (9), 091502.
 Pavez, C., Pedreros, J., Zambra, M., Veloso, F., Moreno, J., Tarifeño, A., Soto, L., 2012. *Plasma Phys. Control. Fusion* 54 (10), 105018.
 Raspa, V., Moreno, C., 2009. *Phys. Lett. A* 373 (40), 3659.
 Raspa, V., Sigaut, L., Llovera, R., Cobelli, P., Knoblauch, P., Vieytes, R., Clausse, A., Moreno, C., 2004. *Braz. J. Phys.* 34 (4b), 1696.
 Raspa, V., Moreno, C., Sigaut, L., Clausse, A., 2007. *J. Appl. Phys.* 102 (12), 123303.
 Raspa, V., Di Lorenzo, F., Knoblauch, P., Lazarte, A., Tartaglione, A., Clausse, A., Moreno, C., 2008. *PMC Phys. A* 2 (1), 5.
 Raspa, V., Knoblauch, P., Di Lorenzo, F., Moreno, C., 2010. *Phys. Lett. A* 374 (46), 4675.
 Tafreshi, M., Golalikhani, M., Sobhanian, S., Jafarizadeh, M., 2010. *J. Phys. Mol.* 1 (2), 25–31.
 Tartari, A., Da Re, A., Mezzetti, F., Angeli, E., De Chiara, P., 2004. *Nucl. Instrum. Methods Phys. Res. Sect. B* 213, 607.
 Venere, M., Moreno, C., Clausse, A., Barbuzza, R., Del Fresno, M., 2001. *Nukleonika* 46 (1), S93.
 Verma, R., Rawat, R.S., Lee, P., Krishnan, M., Springham, S.V., Tan, T.L., 2010. *IEEE Trans. Plasma Sci.* 38 (4), 652.
 Whitlock, R., Dozier, C., Newman, D., Petr, R., Freshman, J., Hoey, D., Heaton, J., 2002. *Proc. SPIE* 4781, 54–60.
 Zapryanov, S., Yordanov, V., Blagoev, A., 2011. *Bulg. J. Phys.* 38, 184–190.